Study of active sites on the MFI zeolite catalysts for the transformation of ethanol into propylene

Wei Xia, Atsushi Takahashi, Isao Nakamura, Hiromichi Shimada, Tadahiro Fujitani*

Research Institute for Innovation in Sustainable Chemistry, National Institute of Advanced Industrial Science and Technology (AIST), Tsukuba West 16-1 Onogawa, Tsukuba, Ibaraki 305-8569, Japan

ABSTRACT

Industrial demand for propylene is increasing. Alternative sources of propylene other than petroleum are of wide interest. The catalytic transformation of bioethanol is a promising avenue for the production of propylene. However, the reaction mechanism and the nature of active sites on the catalyst remained unclear. In this work, MFI-type zeolite catalysts with various Si/Al_2 ratios (73, 97, 128, 176, 207) were prepared by hydrothermal synthesis under atmospheric pressure. We characterized these MFI catalysts by BET surface area measurements, X-ray fluorescence, X-ray diffraction, scanning electron microscopy, temperature programmed desorption of ammonia, and ^{27}Al MAS NMR to understand the effect of the Si/Al_2 ratio. The ethanol conversion reaction was systematically investigated using these catalysts according to the contact time and reaction temperature. The conversion of ethanol yielded similar product distributions over these catalysts at different contact times, indicating that the product distribution has no relationship with the Si/Al_2 ratio. Also, the propylene production rates per acidic site of these catalysts were similar. These results strongly imply that the acidic sites of the different MFI-type zeolite catalysts have the same nature, as well as the same reactivity. The catalytic activity was proportional to the number of acidic sites.

© 2010 Elsevier B.V. All rights reserved.

1. Introduction

As a major chemical intermediate, the production of propylene always attracts broad attention in the industrial and academic research field. Propylene is generally produced by steam thermal cracking of the naphtha from the petroleum. However, due to the global energy crisis and the increasing demand for propylene in the industrial field, much more attention has been paid to alternative resources to petroleum.

Methanol can be obtained in large quantities from fossil fuels like petroleum, nature gas and coal. The process for methanol to gasoline (MTG) and methanol to olefins (MTO), which can be used to produce liquid fuels for the automotive sector or to make olefins suitable for polymerization, has been well established and commercialized since 1980s [1,2]. Ethanol can be produced from renewable sources such as biomass by fermentation. It also has great potential to be a candidate for the source of light olefins such as ethylene and propylene. If the conversion of ethanol to propylene is selective and efficient, propylene can be produced without the utilization of petroleum resources. Therefore, ethanol to olefin (ETO) process has recently received much attention but has not yet been used

in industrial application. Only a few literatures reported the conversion of ethanol or ethylene to olefin. These literatures reported the conversion of ethanol to hydrocarbons over unmodified and metal-modified ZSM-5 catalysts [3–9]. The conversion of ethylene to propylene has also been investigated over SAPO-34 [10] and nickel ion-loaded mesoporous silica catalysts [11]. Recently, LEV zeolite catalyst was also used for the ethanol to olefin reaction [12]. However, as mentioned above, much attention has been paid to mainly synthesize ethylene, gasoline, or aromatic hydrocarbons from ethanol. There are few reports concerning the ethanol to propylene process [8].

The zeolite H-ZSM-5 has been widely used as the active catalyst for various reactions owing to its special pore structure, thermal and hydrothermal stability, acidity, and reactivity. It has long been used for MTO conversion in industry [1,2]. Furthermore, this catalyst was found to be the alternative catalyst for ethanol transformation into hydrocarbons. Understanding the reaction mechanism and active sites of H-ZSM-5 zeolite catalysts is crucial for improving catalytic performance in ethanol conversion; however, the reaction mechanism and the nature of the active sites remain unclear.

Recently, we studied the conversion reaction of ethanol to propylene on H-ZSM-5 zeolite catalysts. In those works, we speculated that a series of MFI-type zeolite catalysts with various Si/Al_2 ratios could be used to explore both the catalytic perfor-

* Corresponding author. Tel.: +81 29 861 8454; fax: +81 29 861 8374.
 E-mail address: t-fujitani@aist.go.jp (T. Fujitani).

mance of these catalysts under various operating conditions and the nature of active sites for the conversion of ethanol to propylene. In this work, we successfully synthesized a series of MFI-type zeolite catalysts with various Si/Al_2 ratios (73, 97, 128, 176, 207) and characterized the catalysts by BET surface area measurements, X-ray fluorescence (XRF), X-ray diffraction (XRD), scanning electron microscopy (SEM), temperature programmed desorption of ammonia (NH_3-TPD), and ^{27}Al MAS NMR to understand the effects of Si/Al_2 ratios. We systematically converted ethanol to propylene over these catalysts at various contact times and reaction temperatures.

2. Experimental

2.1. Preparation of catalyst

A series of MFI-type zeolite catalysts with various Si/Al_2 ratios was synthesized hydrothermally. Colloidal silica (SNOWTECH O) and $Al(NO_3)_3 \cdot 9H_2O$ were used as Si and Al sources, respectively. Tetra-n-propylammonium bromide was used as a template. $Al(NO_3)_3 \cdot 9H_2O$ was first dissolved in the Colloidal Silica, and then NaCl and NaOH were added to get solution A. The template was dissolved in water to get solution B. Solution B was added slowly to solution A with stirring. After the addition was completed, the gel was stirred for at least 30 min to homogenize while being heated to 373 K. Then the hydrothermal conversion was conducted under reflux for 14 days at atmospheric pressure. Finally, the Na-type zeolites were filtered off, washed thoroughly with deionized water until no Cl^- remained in the filtrate, dried at 383 K for 16 h, and calcined at 873 K for 4 h in an air stream to burn off the template remaining in the zeolite crystals.

H-type zeolite catalysts were prepared from Na-type catalysts by the ion-exchange method. The Na-type zeolite catalysts were repeated ion-exchange for 4 times with a 1 M HCl aqueous solution (500 mL) under reflux at 373 K for 7 days. Finally, the product was filtered off, washed with deionized water until no Cl^- remained in the filtrate and dried at 383 K for 16 h. After that, the catalysts were calcined in air at 873 K for 4 h with a heating rate of 4.5 K/min.

2.2. Characterization

Surface areas and pore volumes were determined by the N_2 adsorption-desorption method (BET method) at 77 K by using a volumetric unit (Micromeritics ASAP 2020). Prior to the adsorption measurements, each sample was degassed at 623 K for 10 h under reduced pressure. XRD patterns of the solid products were measured with a powder X-ray diffractometer (Rigaku, RINT 2000) with Cu Kα monochromatized radiation ($\lambda = 0.154178$ nm) at 40 kV and 40 mA. Si/Al_2 ratios of these catalyst samples were determined by XRF (RIGAKU EDXL 300). The crystal morphology was observed by SEM (Jeol-JSM-5600). NH_3-TPD was also used (BEL-CAT-32) to investigate the acidic site properties. Catalyst sample (0.1 g) was placed in a small quartz tube and dried in flowing He (99.99%, 30 mL/min) at 773 K for 1 h. The sample was cooled to 373 K, the
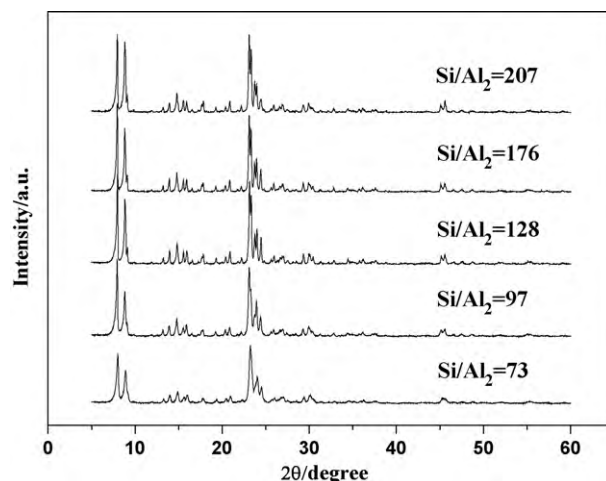

Fig. 1. XRD patterns of the synthesized MFI series of catalysts with various Si/Al_2 ratios.

adsorption of NH_3/He (30 mL/min) for 1 h took place at 373 K, and then the catalyst was flushed with He (30 mL/min) at the same temperature for 1 h to remove NH_3 that was physically adsorbed on the sample surface. TPD measurements were done from 373 to 873 K with a heating rate of 10 K/min, with He as the carrier gas. The desorbed NH_3 was quantified with a thermal conductivity detector. The ^{27}Al MAS NMR spectra were obtained on a Varian VXR-400 spectrometer at 104.3 MHz with a ca. 4.5 kHz spinning speed and 1.73 μs pulses for 4000 scans. The chemical shift was referenced to an external standard of $Al(H_2O)_6^{3+}$.

2.3. Catalytic apparatus and ethanol transformation reaction

Ethanol (99.5%, Wako) was used without further purification. All the MFI zeolite samples were powdered, pressed, crushed, and sieved with a 14–22 mesh. The conversion reaction was carried out at atmospheric pressure using a continuous-flow fixed-bed quartz tubular reactor with 0.1–0.8 g catalyst. Reaction temperature (673–873 K) was monitored by a thermocouple in the catalyst bed. Prior to each reaction, the catalyst was pretreated in a flow
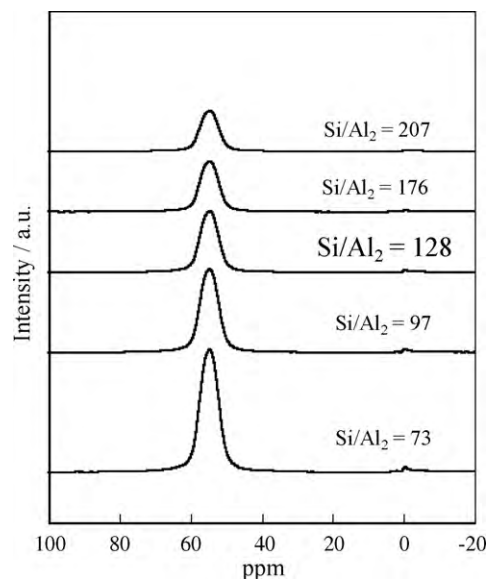
Table 1
Characteristics of MFI-type zeolite catalysts.

Sample no.	Si/Al_2 ratio	BET surface area ($m^2 g^{-1}$)	Pore volume ($cm^3 g^{-1}$)
1	73	371	0.212
2	97	371	0.209
3	128	418	0.202
4	176	379	0.175
5	207	414	0.212

Fig. 2. ^{27}Al MAS NMR spectra of the series of synthesized MFI catalysts with various Si/Al_2 ratios.
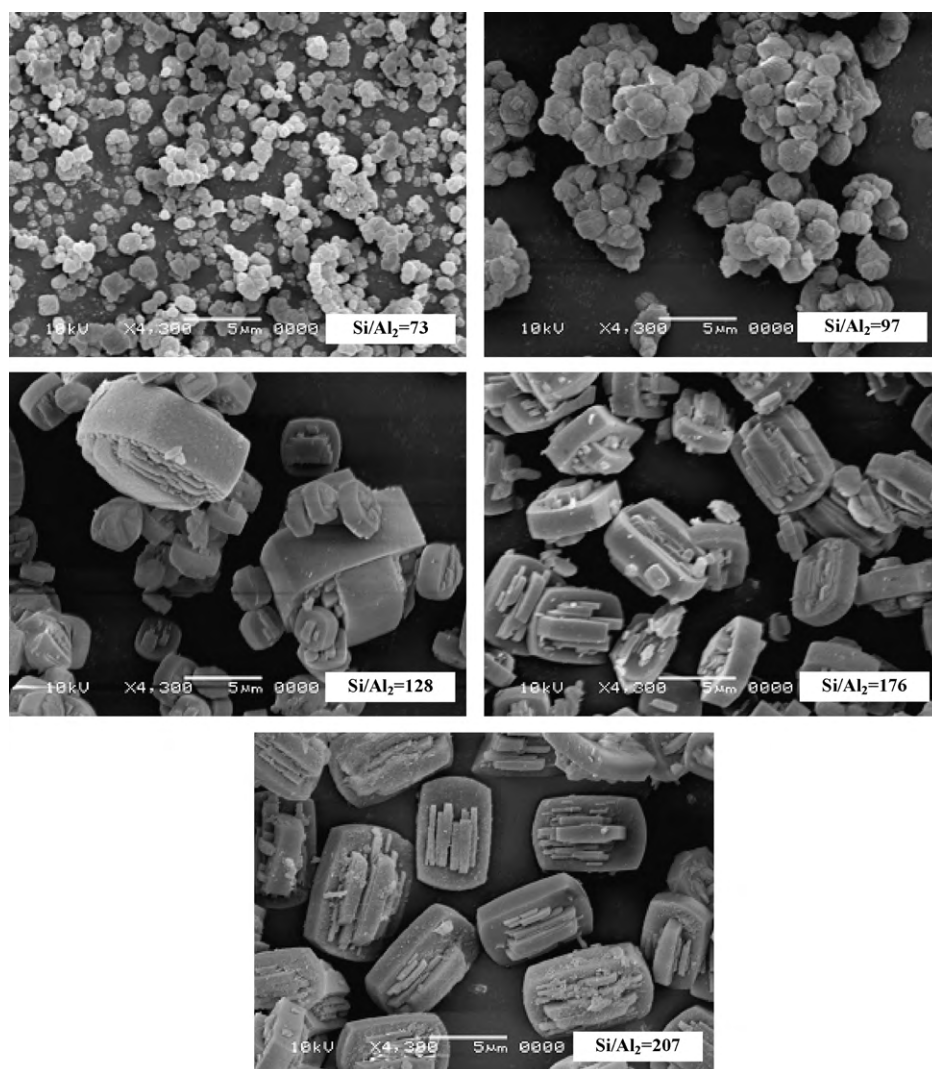
Fig. 3. SEM images of the series of synthesized MFI catalysts with various Si/Al_2 ratios.

of N_2 (flow rate: 100 mL/min) at 873 K for 1 h. Reactants (ethanol concentration 50 vol% in a flow of N_2) were fed into the reactor by means of a micro pump and were vaporized before entering the reactor. The reaction products were analyzed by using on-line gas chromatography (hydrogen-flame ionization detector with RT-alumina PLOT (Restek USA) for C_1–C_4 hydrocarbon, and thermal conductive detector with Shincarbon ST (Shinwa Chem. Ind. Ltd., Japan) for N_2 and H_2).

3. Results and discussion

3.1. Characterization of MFI zeolite catalysts

Table 1 summarizes the XRF and nitrogen adsorption/desorption (BET) results for these MFI zeolite catalysts. The BET surface areas of all the catalysts were between 370 and $420 \, m^2 \, g^{-1}$. The pore volumes of the catalysts were mostly about $0.2 \, cm^3 \, g^{-1}$.

These MFI zeolites were characterized for their crystalline nature by XRD. The XRD patterns of the synthesized MFI zeolites are shown in Fig. 1. All samples' XRD patterns presented similar diffraction peaks, which were consistent with typical X-ray patterns of MFI-type zeolite structure, and no other peak could be observed. The results indicated that the MFI-type catalysts with high purity
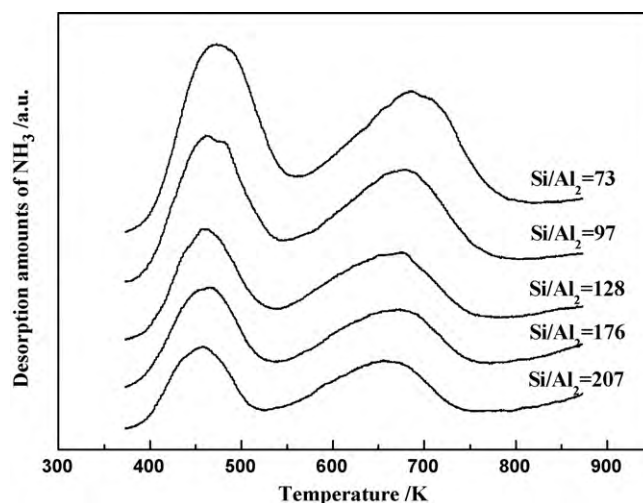

Fig. 4. NH_3-TPD profiles of the series of synthesized MFI catalysts with various Si/Al_2 ratios.
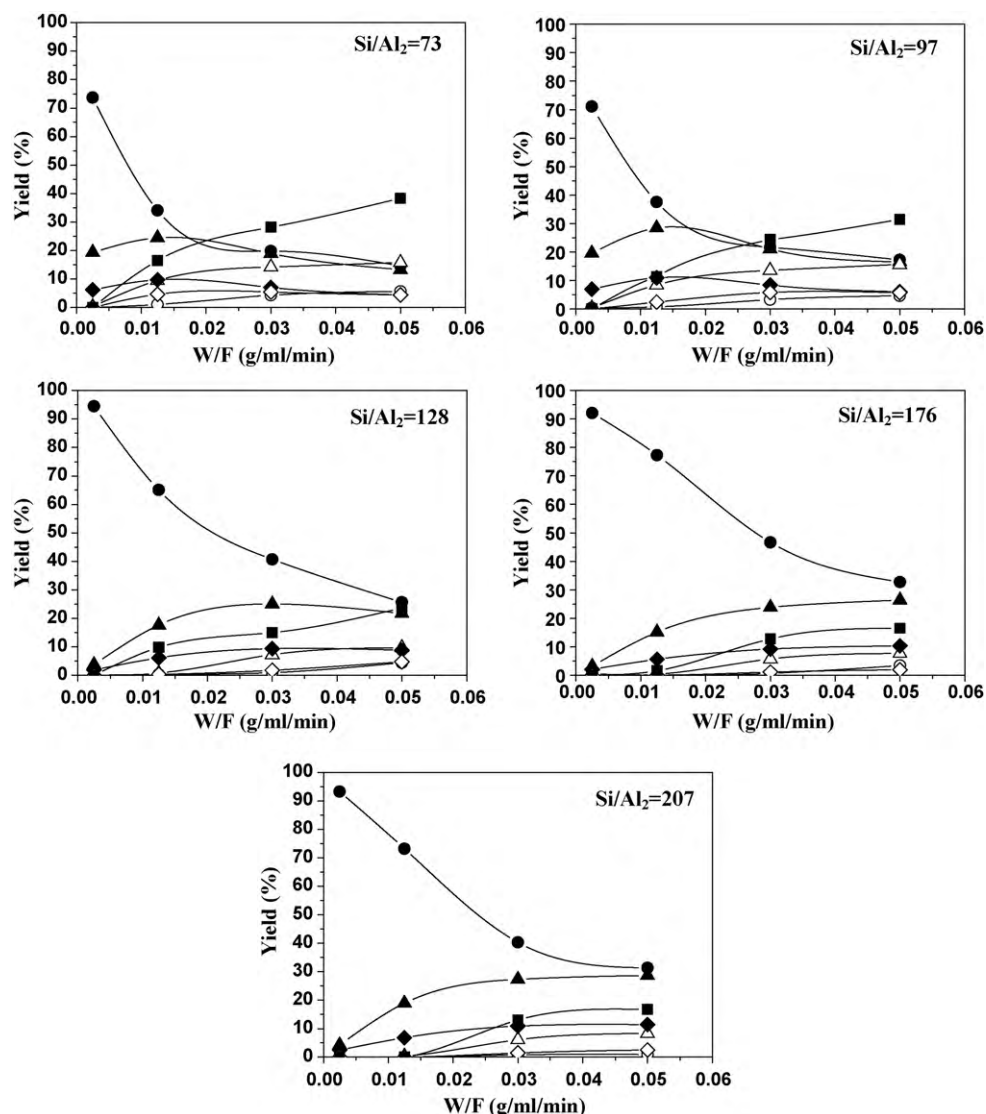
Fig. 5. Product distribution over the series of synthesized MFI catalysts: (●) ethylene, (○) ethane, (▲) propylene, (△) propane, (◆) butene, (◇) butane and (■) others. Reaction conditions: time-on-stream, 30 min; reaction temperature, 823 K; $P = 0.1$ MPa.

were successfully synthesized. As shown in Fig. 1, the XRD patterns have different relative peak intensity. The MFI catalysts with the higher Si/Al_2 ratio showed higher peak intensity.

Fig. 2 displays the ^{27}Al MAS NMR spectra of the catalyst samples with various Si/Al_2 ratios. The peak at 56 ppm is commonly assigned to four-coordinated framework aluminum, while the peak at 0 ppm is referred to non framework octahedral aluminum [13]. As shown in Fig. 2, all the catalyst samples exhibited the same framework aluminum (tetrahedrally coordinated) peaks at about 56 ppm. No nonframework aluminum peak could be observed. The results indicate that all the Al atoms are incorporated into the cat-

alyst framework. Furthermore the intensity of the signal at 56 ppm decreased with increasing Si/Al_2 ratio.

SEM was also used to investigate the crystal size and morphology of these MFI catalyst samples. The micrographs were presented in Fig. 3. Most of these crystals showed the MFI-typical hexagonal morphology. The crystals of the catalyst with $Si/Al_2 = 73$ were smaller than 1 μm. The small crystals of the catalyst with $Si/Al_2 = 97$ tended to form agglomerates around 5–10 μm. The catalyst with $Si/Al_2 = 128$ included some small crystals (smaller than 2.5 μm) together with large crystals (about 10 μm), all with the same shape. The crystals of the catalysts with $Si/Al_2 = 176$ and 207 were similar

Table 2
Ethanol conversion over synthesized MFI catalysts.

Si/Al_2 ratio	W/F	Ethylene	Ethane	Propylene	Propane	Butene	Butane	Others
73	0.0125	34.1	1.0	24.5	9.4	9.7	4.3	16.7
97	0.0125	37.6	0.8	28.4	8.5	11.0	2.4	12.2
128	0.03	40.7	0.9	25.0	7.2	9.3	1.8	15.0
176	0.05	35.6	1.1	25.5	7.6	9.8	1.9	16.5
207	0.05	31.6	1.0	28.6	8.9	11.4	2.5	16.7

Reaction conditions: time-on-stream, 30 min; reaction temperature, 823 K; $P = 0.1$ MPa.
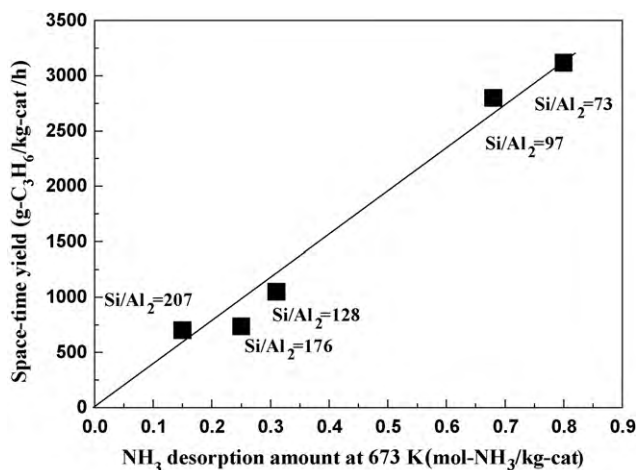
Fig. 6. Correlation between space-time yield and the NH$_3$ desorption amount at high temperature (673 K).

in shape, but the latter were a little larger. Clearly, the Si/Al$_2$ ratio affected the morphology of these MFI catalysts. The crystals size increased with Si/Al$_2$ ratio, a conclusion that is also supported by the XRD peak intensities.

We investigated the amount and strength of acidic sites of the zeolite catalyst series by using the NH$_3$-TPD method (Fig. 4). All the catalyst samples exhibited the same two well-resolved NH$_3$ desorption peaks: the low-temperature peak at about 473 K and the high-temperature peak at about 673 K, corresponding to the weak and strong acid sites, respectively. This result means that the strengths of the acid sites of these MFI catalysts were the same. The spectral peak area decreased with increasing Si/Al$_2$ ratio, which indicates that the density and total amount of acidic sites decreased with increasing Si/Al$_2$ ratio.

3.2. Transformation of ethanol to propylene

Over each of the synthesized MFI-type catalysts, we carried out the ethanol conversion reactions under atmospheric pressure at 673, 723, 773, 823, and 873 K. Under these reaction conditions on these catalysts, ethanol was completely converted to hydrocarbons, such as ethylene, propylene, and other higher hydrocarbons. We compared catalytic performance at various contact times and reaction temperatures. The optimum yield for propylene (at various reaction temperatures) was 24–28%. Fig. 5 shows the production distribution on these catalysts at 823 K. The contact time is defined as W/F, where W denotes the catalyst weight (g) and F denotes the total flow rate (mL/min). As shown in Fig. 5, over all catalysts, ethylene was the main product under very low W/F conditions. As W/F increased, ethylene yield decreased, and propylene and butene yields increased. Paraffins (ethane, propane, and butane) increased with the decrease of olefins (ethylene, propylene, and butene), which were produced by hydrogenating olefin. On the basis of these results, we proposed the reaction mechanism. First, ethylene was produced from ethanol. Then the ethylene was converted in parallel to propylene and butene. Finally, propylene, and butene were converted to propane, butane, and other higher hydrocarbons (olefin, paraffins, and aromatics). The details of the reaction mechanism will be presented in a future report. As shown in Fig. 5, the contact time for optimum propylene yield increased with increasing Si/Al$_2$ ratio, perhaps due to variations in MFI catalyst acidic site density with Si/Al$_2$ ratio: the acidic site density of MFI catalyst with high Si/Al$_2$ ratio was lower than that of catalyst with low Si/Al$_2$ ratio. So the contact time when the optimum propylene yield was obtained was delayed. In addition, in order to develop the catalyst

with high selectivity for ethanol transformation to propylene, it is very important to inhibit the transformation from propylene and butene to over C$_5$ products, which will be further investigated in our future work.

We also further compared and summarized the above product distribution results. At various contact times (W/F), similar product distributions were obtained on all five catalysts (Table 2). This result strongly implies that the product distribution is independent of the Si/Al$_2$ ratio. The nature of acidic sites among H-ZSM-5 catalysts should be the same.

The high-temperature peak acid sites were reported to be connected with the active center for the conversion of methanol [14]. We calculated the number of strong acid sites corresponding to the desorption amount of NH$_3$ at high temperature from the NH$_3$-TPD spectra of our zeolite catalyst series; also, we calculated the initial propylene space-time yield (STY) of these MFI-type catalysts. Fig. 6 showed the relationship between STY and the NH$_3$ desorption amount at high temperature (673 K). The relationship of STY to NH$_3$ desorption amount at the high temperature (673 K) was almost linear; that is, STY increased linearly with the number of strong acid sites. So the strong acid sites are the active sites for the ethanol conversion to propylene. The turnover frequency on each active site was same on the different Si/Al$_2$-ratio catalysts. This indicates that the active sites are the same in nature on the different H-ZSM-5 catalysts. For the ethanol conversion reaction, only the number of active sites on the MFI catalysts changed with Si/Al$_2$ ratio. On the basis of the product distribution and TPD results, we propose that the nature and reactivity of the acidic sites are the same on MFI-type zeolite catalysts with different Si/Al$_2$ ratios.

4. Conclusions

A series of MFI-type zeolite catalysts with various Si/Al$_2$ ratios was successfully synthesized. To understand the effects of Si/Al$_2$ ratios on the catalysts, we characterized them by BET surface area measurements, XRF, XRD, SEM, NH$_3$-TPD and ^{27}Al MAS NMR. The conversion of ethanol over these catalysts at various contact times yielded similar product distributions, which indicates that the product distribution is independent of the Si/Al$_2$ ratio. Also, the production rates of propylene per acidic site of these catalysts were identical. These results strongly imply that the acidic sites on the different MFI-type zeolite catalysts have the same nature and reactivity; the catalytic activity should be proportional to the number of acidic sites.

References

[1] C.D. Chang, A.J. Silvestri, J. Catal. 47 (1977) 249–259.
[2] P. Dejaifve, J.C. Vedrine, V. Bolis, E.G. Derouane, J. Catal. 63 (1980) 331–345.
[3] J. Schulz, F. Bandermann, Chem. Eng. Technol. 17 (1994) 179–186.
[4] A.T. Aguayo, A.G. Gayubo, A.M. Tarrío, J. Bilbao, J. Chem. Technol. Biotechnol. 77 (2002) 211–216.
[5] M. Inaba, K. Murata, M. Saito, I. Takahara, Green Chem. 9 (2007) 638–646.
[6] N.R.C. Fernandes Machado, V. Calsavara, N.G.C. Astrath, A. Medina Neto, M.L. Baesso, Appl. Catal. A 311 (2006) 193–198.
[7] V. Calsavara, M.L. Baesso, N.R.C. Fernandes Machado, Fuel 87 (2008) 1628–1636.
[8] K. Murata, M. Inaba, I. Takahara, J. Jpn. Petrol. Inst. 51 (2008) 234–239.
[9] R. Johansson, S.L. Hruby, J. Rass-Hansen, C.H. Christensen, Catal. Lett. 127 (2009) 1–6.
[10] H. Oikawa, Y. Shibata, K. Inazu, Y. Iwase, K. Murai, S. Hyodo, G. Kobayashi, T. Baba, Appl. Catal. A: Gen. 312 (2006) 181–185.
[11] M. Iwamoto, Y. Kosugi, J. Phys. Chem. C 111 (2007) 13–15.
[12] T. Inoue, M. Itakura, H. Jon, Y. Oumi, A. Takahashi, T. Fujitani, T. Sano, Microporous Mesoporous Mater. 122 (2009) 149–154.
[13] W. Zhang, X. Bao, X. Guo, X. Wang, Catal. Lett. 60 (1999) 89–94.
[14] H. Itoh, C.V. Hidalgo, T. Hattori, M. Niwa, Y. Murakami, J. Catal. 85 (1984) 521–526.